

Report

AtABCG29 Is a Monolignol Transporter Involved in Lignin Biosynthesis

Santiago Alejandro,^{1,5,*} Yuree Lee,^{2,5} Takayuki Tohge,^{3,5,*} Damien Sudre,^{1,5,6} Sonia Osorio,³ Jiyoung Park,⁴ Lucien Bovet,^{1,7} Youngsook Lee,⁴ Niko Geldner,² Alisdair R. Fernie,³ and Enrico Martinoia^{1,4}

¹Institute of Plant Biology, University of Zurich, 8008 Zurich, Switzerland

²Department of Plant Molecular Biology, University of Lausanne, Quartier Sorge, 1015 Lausanne, Switzerland

³Max Planck Institute of Molecular Plant Physiology, Am Muehlenberg 1, 14476 Potsdam, Germany

⁴POSTECH-UZH Cooperative Laboratory, Department of Integrative Bioscience and Biotechnology, Pohang University of Science and Technology, Pohang 790-784, South Korea

Summary

Lignin is the defining constituent of wood and the second most abundant natural polymer on earth. Lignin is produced by the oxidative coupling of three monolignols: *p*-coumaryl alcohol, coniferyl alcohol, and sinapyl alcohol [1]. Monolignols are synthesized via the phenylpropanoid pathway and eventually polymerized in the cell wall by peroxidases and laccases. However, the mechanism whereby monolignols are transported from the cytosol to the cell wall has remained elusive. Here we report the discovery that AtABCG29, an ATP-binding cassette transporter, acts as a *p*-coumaryl alcohol transporter. Expression of *AtABCG29* promoter-driven reporter genes and a *Citrine-AtABCG29* fusion construct revealed that AtABCG29 is targeted to the plasma membrane of the root endodermis and vascular tissue. Moreover, yeasts expressing AtABCG29 exhibited an increased tolerance to *p*-coumaryl alcohol by excreting this monolignol. Vesicles isolated from yeasts expressing AtABCG29 exhibited a *p*-coumaryl alcohol transport activity. Loss-of-function *Arabidopsis* mutants contained less lignin subunits and were more sensitive to *p*-coumaryl alcohol. Changes in secondary metabolite profiles in *abcg29* underline the importance of regulating *p*-coumaryl alcohol levels in the cytosol. This is the first identification of a monolignol transporter, closing a crucial gap in our understanding of lignin biosynthesis, which could open new directions for lignin engineering.

Results and Discussion

Coexpression Analysis of AtABCG29

Lignin is an important component of cell walls that gives structural rigidity to plants. Identification of lignin biosynthetic

genes has attracted much attention during the last decade. All steps of the phenylpropanoid biosynthesis leading to lignin precursors are carried out within the plant cell [2]. However, the last step, polymerization of the monolignols, occurs in the apoplastic space. This requires that monolignols be transported across the plasma membrane, a process that has been recently reported to be an ATP hydrolysis-dependent transport [3]. In order to identify genes involved in monolignol transport, we performed a coexpression network analysis with the ABCG transporter subfamily (previously called WBCs and PDRs) of *Arabidopsis* using the ATTED-II database (<http://atted.jp/>). Members of the ABCG subfamily have been shown to transport a broad range of fatty acids and terpenoids. We therefore wondered whether this class could also be implicated in the transport of phenolic compounds. The results revealed that AtABCG29/PDR1, a member of the full-size ABCG subfamily [4, 5], exhibited a high coexpression ratio with three genes of the phenylpropanoid biosynthesis pathway (see Figure S1 available online), which is involved in the synthesis of lignin and flavonoids [1]. The well-correlated genes correspond to two 4-coumarate coenzyme A (CoA) ligases (4CL2 and 4CL5), which convert hydroxycinnamic acids into hydroxycinnamoyl CoA esters, and one caffeoyl CoA-O-methyltransferase catalyzing the conversion of caffeoyl CoA into feruloyl CoA [6]. Moreover, seven further genes related to phenylpropanoid biosynthesis are coexpressed with AtABCG29, albeit with lower coexpression ratios (Figure S1). In concordance with our data, Ehltling and colleagues [7] reported that AtABCG29 showed an expression pattern in primary stems consistent with that of monolignol biosynthetic genes and increased lignin content. Therefore, these results rendered AtABCG29 a good candidate transporter for monolignol export.

Tissue-Specific Expression and Subcellular Localization of AtABCG29

To investigate tissue-specific expression, we used a 2.2 kb fragment upstream the *AtABCG29* coding sequence to drive the expression of the GUS reporter. GUS activity was detected mainly in the primary and secondary roots, but not in the root tip (Figures 1A–1C). Meristematic cells at the root tip do not deposit lignin; therefore, the expression pattern observed in Figure 1B corresponds to that expected for a monolignol exporter [8]. In addition, in 2-week-old plants no GUS signals were detected in the hypocotyl and the upper part of the primary root (Figure S2A), probably because in this part of the root, monolignol synthesis and deposition are reduced [9, 10]. We also detected GUS expression in the lower part of the stem and whole vasculature of rosette leaves (Figure S2B) and anthers, where the endothecium contains a high level of lignin and siliques (Figures S2C and S2D) [11]. Public microarray data indicate that AtABCG29 is expressed mainly in the roots and stems (http://bar.utoronto.ca/efp_arabidopsis/cgi-bin/efpWeb.cgi), corresponding to the parts of a plant containing a higher amount of lignin [12], whereas expression in flowers and siliques is lower. In order to get a higher resolution of the expression pattern, we fused the 2.2 kb upstream fragment to the 42 kDa fluorescent reporter protein NLS-GFP that contains a classical nuclear localization sequence (NLS) but

⁵These authors contributed equally to this work

⁶Present address: Biochimie et Physiologie Moléculaire des Plantes, CNRS, INRA, Université Montpellier 2, SupAgro. Bat 7, 2 Place Viala, 34060 Montpellier Cedex 1, France

⁷Present address: Philip Morris Products SA, PMI R&D, 2000 Neuchâtel, Switzerland

*Correspondence: saalmar333@hotmail.com (S.A.), tohge@mpimp-golm.mpg.de (T.T.)

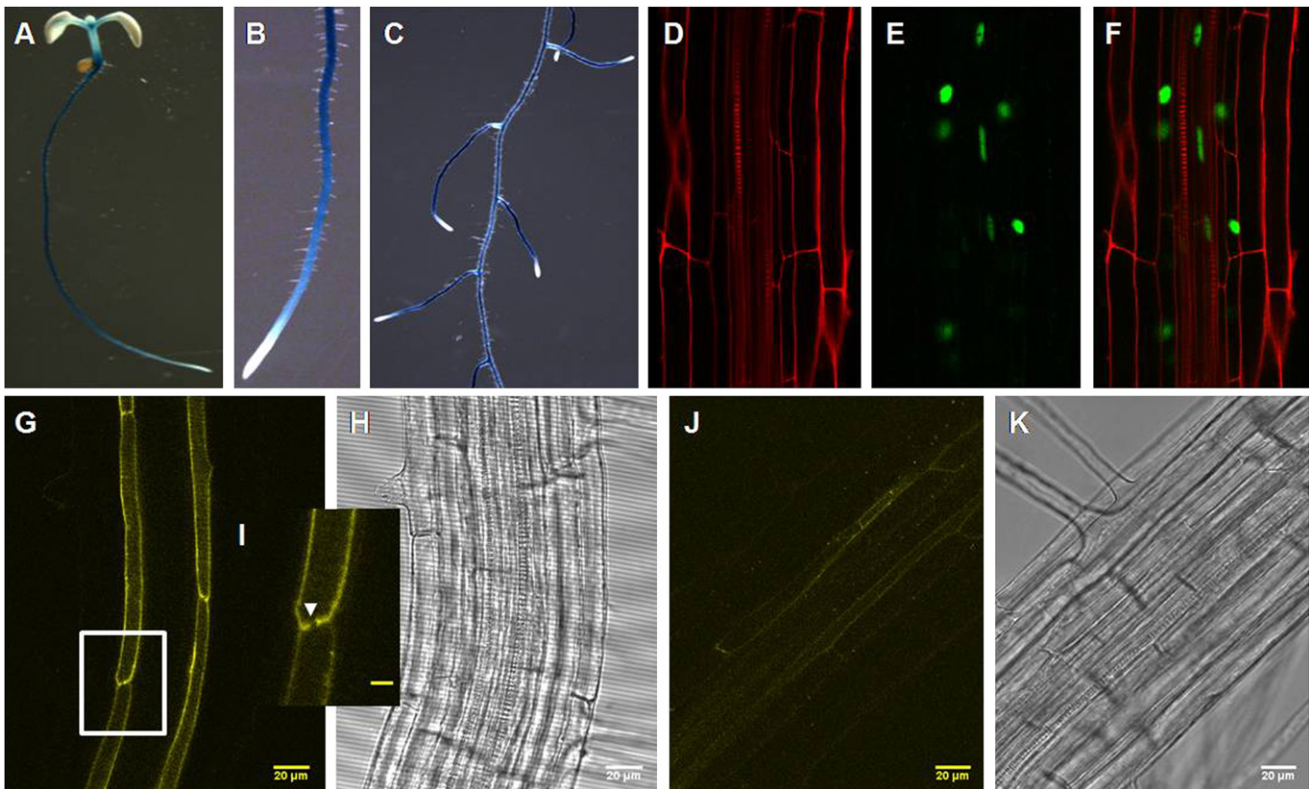


Figure 1. AtABCG29 Is Detected in Vascular Tissue and Plasma Membrane of Endodermal Cells in Roots

(A–C) *AtABCG29* promoter-GUS (*promABCG29::NLS-GFP-GUS*) reporter gene expression in 5-day-old seedling (A) and in 2-week-old plant root (B and C). For tissue localization of *AtABCG29*, a fluorescent reporter protein NLS-GFP driven by the native promoter (*promABCG29::NLS-GFP-GUS*) was used. (D–F) Five-day-old root seedling treated with 10 μ M propidium iodide (D), GFP fluorescence (E), and overlay (F). (G–I) Localization of *Citrine-ABCG29* expression driven by an endodermis-specific promoter *CASP1* (*pCASP1::ABCG29N-Citrine*) in 5-day-old root seedling (G) and under bright-field illumination (H). (I) shows a close-up image of an endodermal cell; the arrowhead indicates the position of the Casparian strip domain. Scale bar in (I) represents 5 μ m. (J and K) *AtABCG29* promoter::*Citrine-ABCG29* (*pABCG29::Citrine-ABCG29*) gene expression in root endodermal cells (J) and bright-field illumination (K). See Figure S2.

lacks nuclear retention or export signals [13]. This construct demonstrated that *AtABCG29* is only expressed in the endodermis and vascular tissue above the elongation zone (Figures 1D–1F). These results are consistent with the *Arabidopsis* Gene Expression Database (AREX) (<http://www.arexdb.org>) and further support the hypothesis that *AtABCG29* might be involved in lignin biosynthesis.

To study the subcellular localization of *AtABCG29*, we fused a yellow fluorescent protein (citrine) to the N terminus of *AtABCG29* (*ABCG29N*) and expressed it under the control of an endodermis-specific promoter (*pCASP1::Citrine-ABCG29N*) [14] and the endogenous promoter (*pABCG29::Citrine-ABCG29N*). Endodermis-specific expression was chosen because the endodermis is the largest and outermost cell layer in which *ABCG29* is endogenously expressed, and *pCASP1* drives strong expression in this cell layer, making it ideal for subcellular localization studies. *Citrine-AtABCG29N* was detected at the plasma membrane of the endodermis except in the Casparian strip domain (CSD) (Figures 1G–1I). The *pABCG29::Citrine-ABCG29N* protein was also detected in the plasma membrane of endodermal cells (Figures 1J and 1K), albeit with a much weaker signal. The fact that the fluorescent signal is interrupted in the CSD, where plasma membrane proteins are excluded [15], indicates that the peripheral *AtABCG29* signal represents indeed plasma membrane and

not cortical ER or the vacuole, in which cases a continuous signal would be expected.

Functional Analysis of the *AtABCG29* Gene Product

The three most abundant monolignols are *p*-coumaryl alcohol, coniferyl alcohol, and sinapyl alcohol. Upon incorporation into the lignin polymer, these monomers are referred to as *p*-hydroxyphenyl (H), guaiacyl (G), and syringyl (S) units, respectively [1, 2]. Because we hypothesized that *AtABCG29* is involved in lignin synthesis acting as a monolignol exporter, we expressed *AtABCG29* in the YMM12 yeast strain that carries loss-of-function mutations in eight ABC transporters. The mutant displays delayed growth even under normal growth conditions (Figure 2A), which was expected because many of the PDRs are important for cellular detoxification and cell fitness during cell growth [16]. We therefore tested the effect of the three monolignols on yeast growth. The addition of coniferyl alcohol to the growth medium decreased the growth rates of YMM12 but also those of the wild-type (WT) and YMM12 expressing *ABCG29* (Figure S3A). No significant effect could be observed in the presence of sinapyl alcohol in any strain tested (Figure S3B). In contrast, whereas upon exposure to *p*-coumaryl alcohol, growth of the WT yeast was not affected, that of YMM12 was strongly retarded compared to that on control medium. YMM12 expressing *AtABCG29*

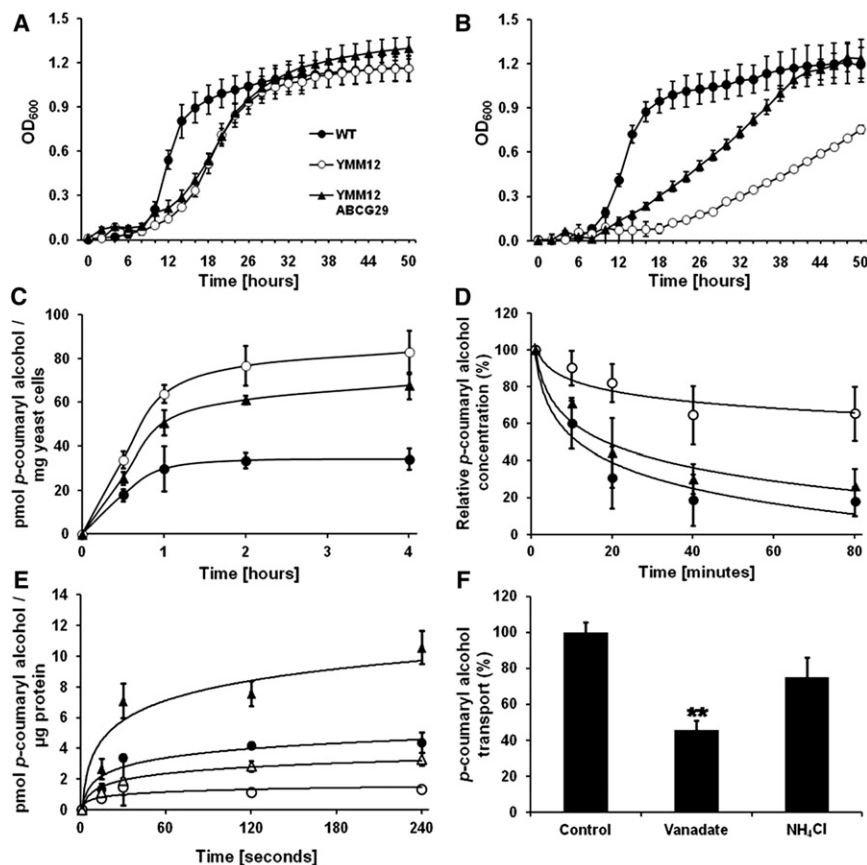


Figure 2. Growth Inhibition by *p*-Coumaryl Alcohol of a Yeast ABC Transporter Mutant Is Rescued by Expression of AtABCG29 that Mediates the Efflux of *p*-Coumaryl Alcohol

(A and B) Growth of wild-type yeast (YPH449, WT), a mutant strain with the empty pNEV vector (YMM12), and an *AtABCG29*-overexpressing mutant strain (YMM12 ABCG29) was monitored. The yeast cells were grown in SCD (A) or SCD + 3 mM *p*-coumaryl alcohol (B). The growth curves are derived from the mean values of four independent cultures for each time point. The experiment was repeated three times with similar results.

(C) *p*-coumaryl alcohol accumulation. Cells from WT yeast (▲) mutant strain with the empty pNEV vector (○) and *AtABCG29* overexpression (●) were grown overnight in SCD, and 2 mM *p*-coumaryl alcohol was added at time 0.

(D) *p*-coumaryl alcohol efflux. Cells from the yeast strains described for (A) were loaded with 2 mM *p*-coumaryl alcohol for 1.5 hr at 4°C, washed, and resuspended in *p*-coumaryl alcohol-free SCD medium at time 0. Data are presented as the percentage of *p*-coumaryl alcohol concentration at time 0. Actual values of this 100% (time point 0) were 5.6, 8.7, and 4.7 pmol *p*-coumaryl alcohol/mg yeast cells by WT, YMM12, and YMM12 ABCG29, respectively.

(E) Time-dependent *p*-coumaryl alcohol uptake into microsomes. For non-ATP-dependent uptake, the reaction mix lacked ATP. ○, pNEV - ATP; ●, pNEV + ATP; △, pNEV-*AtABCG29* - ATP; ▲, pNEV-*AtABCG29* + ATP.

(F) Inhibition of *AtABCG29* transport by 1.5 mM vanadate and 5 mM NH₄Cl (control, without inhibitor). Results are the mean values of three independent cultures for each time point. The experiments were repeated four times with similar results. ***p* < 0.01.

All error bars are SD calculated from three technical replicates. See Figure S3.

exhibited an intermediary phenotype, indicating that this ABCG protein was able to export *p*-coumaryl alcohol and reduce its toxic effect in yeast (Figure 2B). In order to gain further proof as to whether *AtABCG29* acts as a *p*-coumaryl alcohol transporter, we performed time-dependent loading and unloading assays. Yeasts expressing *AtABCG29* accumulated less *p*-coumaryl alcohol than the empty vector control (Figure 2C). Our hypothesis could be confirmed by performing efflux analysis from preloaded yeasts. Whereas *p*-coumaryl alcohol was only slowly released from YMM12 cells, both WT and *AtABCG29*-expressing cells efficiently released *p*-coumaryl alcohol (Figure 2D). The transport of *p*-coumaryl alcohol by ABCG29 transporter appears to be substrate specific because no differences were observed in loading and unloading analysis of sinapyl or coniferyl alcohol in yeast cells (data not shown). ABCG29-expressing yeasts export amounts of *p*-coumaryl alcohol similar to their corresponding WT despite that they grow more slowly in the presence of this monolignol. This can be explained by the fact that growth of the multiple mutant is not only affected by *p*-coumaryl alcohol (Figure 2A). Further evidence that *AtABCG29* acts as a *p*-coumaryl alcohol transporter was obtained by performing transport experiments with yeast microsomes. The efflux activity observed in yeast cells can be detected as *p*-coumaryl alcohol uptake after the addition of MgATP because the membrane isolation results in a mixed population of right-

side-out and inside-out vesicles. The uptake of *p*-coumaryl alcohol into yeast vesicles was strongly increased in vesicles isolated from *AtABCG29*-expressing yeasts (Figure 2E). The residual transport activity may be due to diffusion or to an intrinsic low-capacity transporter [17]. Furthermore, vanadate, which is an effective inhibitor of ABC transporters, inhibited the ATP-dependent *p*-coumaryl alcohol uptake by more than 60%, whereas NH₄Cl, which abolishes the transmembrane H⁺ gradients, exhibited a negligible inhibitory effect (Figure 2F). To test whether ABCG29 could transport other components of lignin biosynthesis, we performed further transport experiments with yeast microsomes. The uptake of sinapyl alcohol was slightly increased (Figure S3C), but no differences were observed for coniferyl alcohol, cinnamic acid, ferulic acid, or caffeic acid (data not shown). These results strongly suggest that *AtABCG29* represents a *p*-coumaryl alcohol exporter that may have some minor activity toward sinapyl alcohol.

Phenotype of *abcg29* Mutant Lines

To obtain further evidence that *AtABCG29* acts also as a *p*-coumaryl alcohol exporter in planta, we tested whether *abcg29* knockout mutants are more sensitive to toxic concentrations of *p*-coumaryl alcohol. We identified two T-DNA insertion lines for *AtABCG29* in the SALK collection (SALK_081047, *abcg29-1* and SALK_102381, *abcg29-2*) (Figure 3A). Using these seeds, we isolated two homozygous loss-of-function

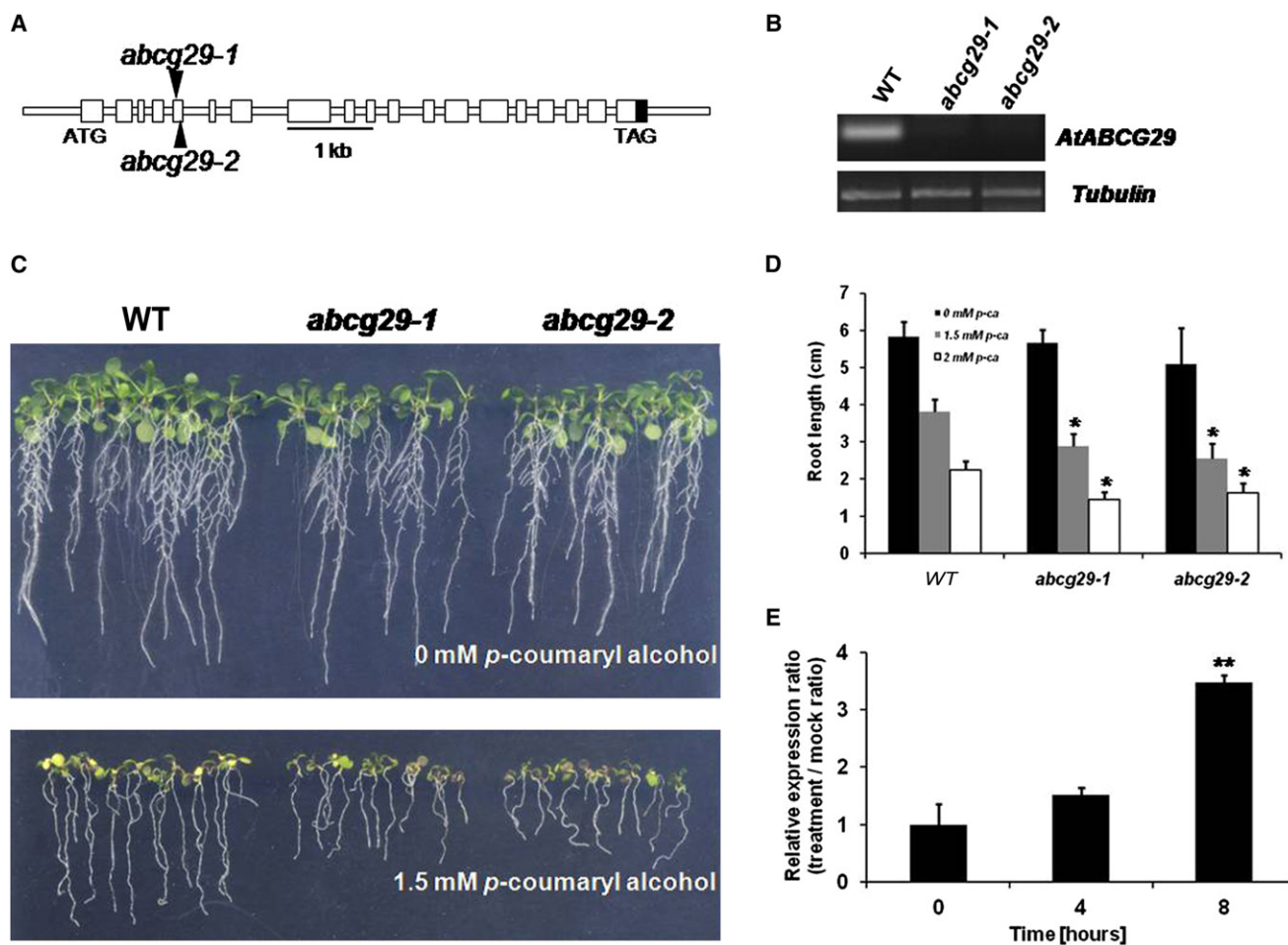


Figure 3. AtABC29 Confers Resistance against Toxicity Effects of *p*-Coumaryl Alcohol and Is Upregulated by This Substrate
 (A) Positions of the insertion in the T-DNA of *atabcg29*. Filled box and open boxes represent the 3' untranslated region and exons of the gene, respectively. Insertions were at the fifth exon. ATG, initial codon; TAG, stop codon.
 (B) *AtABC29* transcript levels in WT and mutant lines determined by semi-quantitative real-time PCR. Total RNA was extracted using TRIzol reagent. cDNAs were synthesized using an RT-PCR kit (Promega) with M-MLV reverse transcriptase.
 (C) Inhibition of plant growth by *p*-coumaryl alcohol. Plants were grown in half-strength MS medium for 2 weeks under long-day conditions (16:8) at 22°C. WT plants were Col-0.
 (D) Primary root lengths of 2-week-old seedlings grown on medium supplemented with 1.5 or 2 mM *p*-coumaryl alcohol ($n > 15$).
 (E) Transcript levels of *AtABC29* in root seedlings treated with 5 mM *p*-coumaryl alcohol. RNA was extracted from roots of 2-week-old seedlings grown in liquid culture. Total RNA was extracted using TRIzol reagent. cDNAs were synthesized using an RT-PCR kit (Promega) with M-MLV reverse transcriptase. Transcript levels were quantified by quantitative real-time PCR. To amplify *AtABC29* cDNA, we performed PCR using the specific primers 5'-TCCGAAATGGTGGATATGGTA-3' and 5'-TGCCAAAAGCAAACATAAACG-3' and *Tubulin* primers 5'-CCTGATAACTTCGCTTTGG-3' and 5'-GTGAACCTCATCTCGTCAT-3'.
 For (D) and (E), results are the mean values of three independent experiments. Experiments were repeated three times with similar results. * $p < 0.05$, ** $p < 0.01$. All error bars are SD calculated from three technical replicates.

mutants (Figure 3B). When plants were grown on *p*-coumaryl alcohol-supplemented medium, root lengths of the loss-of-function mutants were significantly shorter than those of the WT plants (Figures 3C and 3D). No significant growth difference could be observed on control Murashige and Skoog (MS) agar plates. To determine whether *AtABC29* is involved in resistance to other components of lignin biosynthesis, we grew *abcg29* loss-of-function mutant plants on media containing sinapyl alcohol, coniferyl alcohol, cinnamic acid, ferulic acid, or caffeic acid; however, the growth rates were not different from those of WT plants (data not shown). In plants, ABCGs are very often upregulated by their substrate. Therefore, we performed a quantitative real-time PCR analysis for *AtABC29* RNA levels upon exposition of 5 mM *p*-coumaryl,

sinapyl, or coniferyl alcohol. Whereas a 3.5-fold upregulation was observed for plants exposed to *p*-coumaryl alcohol after 8 hr (Figure 3E), no differences were detected for sinapyl or coniferyl alcohol (data not shown). These results further underline the importance of *AtABC29* in exporting *p*-coumaryl alcohol.

Differential Accumulation of Monolignols and Nontargeted Metabolite Profiling

At this point, it was important to determine whether the absence of *AtABC29* has an impact on lignin contents or monolignol composition. To answer this question, we used targeted gas chromatography-mass spectrometry (GC-MS) metabolite profiling of thioacydolyzed roots [18, 19]. Using

Table 1. Changes in the Contents of Lignin Thioacidolysis Products in *abcg29* Mutant Lines, as Identified by GC-MS

	WT	<i>abcg29-1</i>	<i>abcg29-2</i>
<i>p</i> -hydroxyphenyl	11.0 ± 0.6	7.7 ± 1.0*	8.5 ± 0.3**
guaiacyl	112.9 ± 4.5	85.9 ± 9.8*	87.7 ± 1.3**
syringyl	5.6 ± 0.6	3.8 ± 0.5*	3.9 ± 0.3*

Data are presented as nmol/g fresh weight ± SE. Relative peak areas of erythro and threo forms are summarized and used for evaluation of unit levels of *p*-hydroxyphenyl (H), guaiacyl (G), and syringyl (S) forms. Analysis was conducted with four independent biological replicates. **p* < 0.05, ***p* < 0.01.

this approach, we succeeded in obtaining highly reproducible results. Interestingly, not only the H content but also G and S were significantly reduced in the *abcg29* knockout mutants by 23% and 32%, respectively (Table 1). In WT as well as in mutant plants, G was by far the predominant constituent, whereas low levels of both H and S units constituted only approximately 8% and 5%, respectively, of the total lignin (Table 1). These data are not in concordance with the accepted idea that lignin of angiosperms consists mainly of G and S units and a low content of H subunit [2]. Based on the transport specificity of AtABCG29 for H (Figures 2 and 3), we could hypothesize that altered export of *p*-coumaryl alcohol can affect biosynthesis and/or transport of coniferyl and sinapyl alcohol, thus resulting in an overall effect on lignin synthesis. The fact that despite a reduction in lignin contents we could not observe a phenotype is not surprising because it was shown that plants with less lignin, with changes in the H/G/S proportion, or with the presence of other phenolic compounds in the lignin composition show little or no obvious phenotypic effects [2, 20, 21]. The observation that the amount of G and S, monolignols that are not transported or are only marginally transported by ABCG29, is decreased raised the question of whether other metabolites were also affected in this mutant. To answer this question, we performed unbiased metabolite analyses using GC-MS and liquid chromatography-mass spectrometry (LC-MS). Interestingly, the levels of flavonols and aliphatic glucosinolates in the *abcg29* mutant lines are much lower than in WT (Figure S4A). In a more detailed experiment, the lower part of plantlets was divided into three parts—root tip, main root, and hypocotyls—and the resulting sections were analyzed separately. In the root tip and hypocotyls, only slight changes in flavonol and glucosinolate contents were observed when compared to WT. By contrast, we observed a strong decrease of these metabolites in the midpart (Figure S4B). The changes in the flavonol and glucosinolate profiles are well correlated with the expression of ABCG29 in roots (Figure 1). When assessed at the individual metabolite level, *abcg29-1* and *abcg29-2* had reduced levels in the roots of quercetin (Q)- and kaempferol (K)-derived flavonoids [22], anthocyanin 9 (A9), sinapoyl malate, and sinapoyl glucose [23] and five aliphatic and three indole glucosinolates [24]. In contrast, only minor changes could be observed for primary metabolites, and most of these changes were not conserved across both mutants. To verify whether AtABCG29 could also act as a flavonoid transporter, we performed experiments with kaempferol and kaempferol-3-O-glucoside but could not detect any transport activity for these substrates (data not shown). Interestingly, affecting glucosinolate biosynthesis has been shown to result in an altered pattern of phenylpropanoids [25]. The metabolite profiling results suggest that decreased transport activity of *p*-coumaryl alcohol in the

absence of AtABCG29 can regulate levels of diverse secondary metabolites in direct and indirect ways. To gain more evidence for this hypothesis, we performed quantitative real-time PCR analysis for several genes coding for enzymes of the pathways where altered metabolite levels were observed. This revealed that phenylammonia lyase (PAL1), chalcone synthase (CHS), and anthranilate synthase (ASB1), key enzymes for the production of phenolic compounds, flavonoids, and glucosinolates, respectively, were consistently decreased (Figure S4C).

In summary, our experiments using yeasts and plants strongly suggest that AtABCG29 is a *p*-coumaryl alcohol exporter. It may also play a minor role for sinapyl alcohol export. Analysis of the lignin constituents showed that in *abcg29* mutants, not only *p*-hydroxyphenyl is present at lower amounts but also guaiacol and syringyl as well as a large number of flavonoids and glucosinolates. Quantitative real-time PCR analysis indicates that impaired export of *p*-coumaryl alcohol has a large impact on the complete metabolic pathway of phenolics and glucosinolates and hence that the network and crosstalk of this metabolic network may be even more complex than assumed [26, 27]. Nevertheless, identification of ABCG29 as a *p*-coumaryl transporter adds a new layer to our understanding of lignin biosynthesis and, together with the discovery of additional monolignol transporters, could represent an important entry point for future manipulations of this pathway.

Supplemental Information

Supplemental Information includes four figures and Supplemental Experimental Procedures and can be found with this article online at doi:10.1016/j.cub.2012.04.064.

Acknowledgments

This work has been supported by the Spanish Ministry of Science and Innovation (MICINN) (S.A.), a grant of the Staatssekretariat für Bildung und Forschung within the COST action 859 (E.M.), the Swiss National Foundation (E.M.), the Global Research Laboratory program of the Ministry of Education, Science and Technology of Korea grant K20607000006 (Youngsook Lee and E.M.), and the Max Planck Society (T.T. and A.R.F.).

Received: September 15, 2011

Revised: March 15, 2012

Accepted: April 23, 2012

Published online: June 14, 2012

References

- Boerjan, W., Ralph, J., and Baucher, M. (2003). Lignin biosynthesis. *Annu. Rev. Plant Biol.* 54, 519–546.
- Bonawitz, N.D., and Chapple, C. (2010). The genetics of lignin biosynthesis: connecting genotype to phenotype. *Annu. Rev. Genet.* 44, 337–363.
- Miao, Y.C., and Liu, C.J. (2010). ATP-binding cassette-like transporters are involved in the transport of lignin precursors across plasma and vacuolar membranes. *Proc. Natl. Acad. Sci. USA* 107, 22728–22733.
- Verrier, P.J., Bird, D., Burla, B., Dassa, E., Forestier, C., Geisler, M., Klein, M., Kolukisaoglu, U., Lee, Y., Martinoia, E., et al. (2008). Plant ABC proteins—a unified nomenclature and updated inventory. *Trends Plant Sci.* 13, 151–159.
- van den Brûle, S., and Smart, C.C. (2002). The plant PDR family of ABC transporters. *Planta* 216, 95–106.
- Davin, L.B., Jourdes, M., Patten, A.M., Kim, K.W., Vassão, D.G., and Lewis, N.G. (2008). Dissection of lignin macromolecular configuration and assembly: comparison to related biochemical processes in allyl/propenyl phenol and lignan biosynthesis. *Nat. Prod. Rep.* 25, 1015–1090.

7. Ehltng, J., Mattheus, N., Aeschliman, D.S., Li, E., Hamberger, B., Cullis, I.F., Zhuang, J., Kaneda, M., Mansfield, S.D., Samuels, L., et al. (2005). Global transcript profiling of primary stems from *Arabidopsis thaliana* identifies candidate genes for missing links in lignin biosynthesis and transcriptional regulators of fiber differentiation. *Plant J.* **42**, 618–640.
8. Rogers, L.A., and Campbell, M.M. (2004). The genetic control of lignin deposition during plant growth and development. *New Phytol.* **164**, 17–30.
9. Benfey, P.N., and Schiefelbein, J.W. (1994). Getting to the root of plant development: the genetics of *Arabidopsis* root formation. *Trends Genet.* **10**, 84–88.
10. Dolan, L., and Roberts, K. (1995). Plant development: pulled up by the roots. *Curr. Opin. Genet. Dev.* **5**, 432–438.
11. Yang, C., Xu, Z., Song, J., Conner, K., Vizcay Barrena, G., and Wilson, Z.A. (2007). *Arabidopsis* MYB26/MALE STERILE35 regulates secondary thickening in the endothecium and is essential for anther dehiscence. *Plant Cell* **19**, 534–548.
12. Goujon, T., Sibout, R., Eudes, A., MacKay, J., and Jouanin, L. (2003). Genes involved in the biosynthesis of lignin precursors in *Arabidopsis thaliana*. *Plant Physiol. Biochem.* **41**, 677–687.
13. Stochaj, U., Rassadi, R., and Chiu, J. (2000). Stress-mediated inhibition of the classical nuclear protein import pathway and nuclear accumulation of the small GTPase Gsp1p. *FASEB J.* **14**, 2130–2132.
14. Roppolo, D., De Rybel, B., Tendon, V.D., Pfister, A., Alassimone, J., Vermeer, J.E., Yamazaki, M., Stierhof, Y.D., Beeckman, T., and Geldner, N. (2011). A novel protein family mediates Casparian strip formation in the endodermis. *Nature* **473**, 380–383.
15. Alassimone, J., Naseer, S., and Geldner, N. (2010). A developmental framework for endodermal differentiation and polarity. *Proc. Natl. Acad. Sci. USA* **107**, 5214–5219.
16. Jungwirth, H., and Kuchler, K. (2006). Yeast ABC transporters—a tale of sex, stress, drugs and aging. *FEBS Lett.* **580**, 1131–1138.
17. Nagy, R., Grob, H., Weder, B., Green, P., Klein, M., Frelet-Barrand, A., Schjoerring, J.K., Brearley, C., and Martinoia, E. (2009). The *Arabidopsis* ATP-binding cassette protein AtMRP5/AtABCC5 is a high affinity inositol hexakisphosphate transporter involved in guard cell signaling and phytate storage. *J. Biol. Chem.* **284**, 33614–33622.
18. Lapierre, C., Pollet, B., and Rolando, C. (1995). New insights into the molecular architecture of hardwood lignins by chemical degradative methods. *Res. Chem. Intermed* **21**, 397–412.
19. Lapierre, C., Pollet, B., Petit-Conil, M., Toval, G., Romero, J., Pilate, G., Leplé, J.-C., Boerjan, W., Ferret, V., De Nadai, V., and Jouanin, L. (1999). Structural alterations of lignins in transgenic poplars with depressed cinnamyl alcohol dehydrogenase or caffeic acid O-methyltransferase activity have an opposite impact on the efficiency of industrial kraft pulping. *Plant Physiol.* **119**, 153–164.
20. Liu, C.J., Miao, Y.C., and Zhang, K.W. (2011). Sequestration and transport of lignin monomeric precursors. *Molecules* **16**, 710–727.
21. Vanholme, R., Morreel, K., Ralph, J., and Boerjan, W. (2008). Lignin engineering. *Curr. Opin. Plant Biol.* **11**, 278–285.
22. Santelia, D., Henrichs, S., Vincenzetti, V., Sauer, M., Bigler, L., Klein, M., Bailly, A., Lee, Y., Friml, J., Geisler, M., and Martinoia, E. (2008). Flavonoids redirect PIN-mediated polar auxin fluxes during root gravitropic responses. *J. Biol. Chem.* **283**, 31218–31226.
23. Hause, B., Meyer, K., Viitanen, P.V., Chapple, C., and Strack, D. (2002). Immunolocalization of 1- O-sinapoylglucose:malate sinapoyltransferase in *Arabidopsis thaliana*. *Planta* **215**, 26–32.
24. Petersen, B.L., Chen, S., Hansen, C.H., Olsen, C.E., and Halkier, B.A. (2002). Composition and content of glucosinolates in developing *Arabidopsis thaliana*. *Planta* **214**, 562–571.
25. Hemm, M.R., Ruegger, M.O., and Chapple, C. (2003). The *Arabidopsis* *ref2* mutant is defective in the gene encoding CYP83A1 and shows both phenylpropanoid and glucosinolate phenotypes. *Plant Cell* **15**, 179–194.
26. Yan, X., and Chen, S. (2007). Regulation of plant glucosinolate metabolism. *Planta* **226**, 1343–1352.
27. Besseau, S., Hoffmann, L., Geoffroy, P., Lapierre, C., Pollet, B., and Legrand, M. (2007). Flavonoid accumulation in *Arabidopsis* repressed in lignin synthesis affects auxin transport and plant growth. *Plant Cell* **19**, 148–162.